



## Non-linear Geostatistics Approach for An Integrated Surface Mapping in Epithermal Gold Deposit, Lampung

Received 28th March 2021

Accepted 16th June 2021

Published 1st July 2021

Open Access

DOI: 10.35472/jsat.v5i2.444

Linda Permata

Kelompok Keilmuan Eksplorasi Sumberdaya Bumi, Program Studi Teknik Pertambangan, Institut Teknologi Sumatera

Email : [linda.permata@ta.itera.ac.id](mailto:linda.permata@ta.itera.ac.id)

**Abstract:** A conventional surface mapping is calculated by any means of linear interpolator such as nearest neighborhood point (NNP), inverse distance (IDW)/inverse distance square (IDS), polygon, contour weighing, Ordinary Kriging (OK). The latter is included in geostatistic methods and provides more advanced weighing method that differs from the rest. Although OK provides smoothing over mapping data but it does not cover categorial (non-value) data. Besides, it is not best in strongly skewed data that are common in exploration data and is limited to the expected value at some location. On the other hand, a non-linear interpolator is conducted to estimate the conditional expectation at a location, that not only to simply predict the grade or other parameter itself, but also the probability of the parameter at a location with known nearby samples. An integrated surface mapping should have many kinds of data that can be categorized into continuous data (grade, thickness, elevation, etc.) and categorial data (lithology, alteration, structural data, etc.). In order to create a block that consist of all data available in a given deposit, a non-linear transformation will be conducted to estimate values at determined thresholds by Kriging methods, known as Indicator Kriging method and its variants.

**Keywords:** conditional expectation, geostatistics, indicator kriging, integrated mapping, non-linear interpolator

**Abstrak:** Metode pemetaan konvensional hanya melibatkan pembobotan dan interpolator linier. Pembobotan konvensional meliputi *nearest neighborhood point* (NNP), *inverse distance* (IDW)/*inverse distance square* (IDS), poligon, dan kontur, sedangkan pembobotan non-konvensional menggunakan pembobotan Kriging. *Ordinary Kriging* (OK) sebagai salah satu metode linier memiliki kelebihan seperti peta sebaran *smoothed* namun tidak bisa mengolah data kategorial seperti jenis litologi, alterasi, tipe urat, keterdapatan struktur, dan sebagainya. Selain itu, metode linier ini tidak cocok untuk pengolahan data dengan distribusi tidak normal. Di sisi lain, suatu transformasi non-linier dapat dilakukan untuk data kontinu maupun kategorial untuk mengestimasi nilai pada ambang batas yang ditentukan (*Indicator Kriging*/IK dan variannya). Transformasi non-linier akan menghasilkan distribusi bersyarat pada suatu lokasi dari sampel-sampel sekitar yang diketahui. Distribusi tersebut dapat dikonversi menjadi nilai – seperti hasil akhir estimasi dengan interpolator linier – atau berupa probabilitas suatu kadar atau parameter lain pada suatu lokasi, hasil dari parameter sampel lain yang diketahui. Sebuah pemetaan non-konvensional pada suatu tipe endapan akan melibatkan berbagai variabel sehingga untuk membentuk pemetaan yang integratif, pendekatan non-linier lebih efektif untuk memproses variabel kontinu maupun kategorial pada satu blok yang sama.

**Kata Kunci :** distribusi bersyarat, geostatistik, *indicator kriging*, interpolator non-linier, pemetaan integratif

### Introduction

In the preliminary stage of exploration, a broad spectrum of exploration methods is conducted; remote sensing [1] and airborne geophysics [2], [3] are usually used prior to geochemistry [4], detailed ground mapping, and drilling [5]. All methods are intended to give the direction of interest in the prospected area(s), e.g. geophysical method that making use of gold lodes and host rocks conductivity contrast [3] to locate prospect area showing those contrasts. Thus, by

focusing on the area of interest, more evidences will lead to the deposit itself [6]. Nevertheless, the data obtained from every method are unique; one is vast and has high resolution, and one is localised, erratic or widely ranged; one is quantified by numbers, and the other is non-value or categorial data.

The local nature of data is common in any mineral resources exploration since from the beginning, an anomaly is expected – whether lower or higher anomalies – to distinguish from background and decide

the next stage. The problem comes when exploration mapping uses conventional methods – nearest neighborhood, inverse distance/inverse power of distance, polygon, contour area (isograde/isopach), etc. [7], [8] – of which weights do count on other than the data distance and the erratic and localised nature of the data. At this point, manual anomaly mapping from experts can cover the data nature but it sure is scientifically subjective and time consuming.

A more sophisticated method for weighing is introduced and known as ‘Kriging’ [6], [9], [10]. This method consists of various kinds of linear and non-linear approaches. A non-linear approach will be conducted throughout this research to estimate categorial data which do not have values, and continuous data which have values as a comparison to other conventional methods. Previously, researchers have shown linear approach uses to conduct resource/reserve estimations such as metal grades, coal qualities, and soil gas concentrations in geothermal field [11]–[14]. A non-linear approach has been used by previous researchers as well in an epithermal gold resource estimation, having structurally complex gold lodes, veinlets, and stockworks [15], similar to this research’s geological background – except that it was applied directly to mineralization (gold grade), not in an exploration stage where surface maps are essential to guide further exploration activity showing complex structural background, lithology types, geochemical features, that are featured in the case study.

The study will show how the non-linear transformation handles both categorial and continuous data in order to estimate transformed values at each thresholds. The ‘threshold’ can be treated as the cut-off-grade in mining process (for continuous data) or in terms of data grouping (for categorial data), e.g. lithology types, alteration groups, vein textures, etc. The Kriging weight that is applied to the non-linear transformation is known as ‘Indicator Kriging’. The broad spectrum of data obtained from many exploration method (remote sensing, geophysics, geochemistry, trenching, drilling, etc.) can be treated purposefully and quantitatively with this non-linear Kriging method.

## Data

This data is taken from a mountainous area in Tanggamus, Lampung province that is prospected to epithermal gold deposit. Therefore, preliminary exploration in the form of surface mapping is crucial. This surface maps, especially the

geological map and alteration map, are typically done subjectively. The data used to represent the two separate characteristics of data, as well as representing the indirect exploration methods, i.e. remote sensing, geophysics, and geochemistry; and direct exploration methods, i.e. grab sampling and trenches, are as follows.

1. Digital Elevation Model (DEM), lineaments from Garwin (2012), and airborne residual aeromagnetic survey.
2. Outcrop sampling, from surface mapping, comprises lithology type and alteration group.

The data obtained are presented in **Figure 1** contains a contour map derived from DEM, lineament density, residual aeromagnetic anomaly (RGB format), XRD sampling points (for analysing alteration group), and observation points from which lithology types are taken. Direct exploration methods was conducted in the area of interest because it covers both high and low anomalies of aeromagnetic survey as well as what is suspected to be the depression of the northern tail of East Semangko pull-apart basin (SPB). This regional structural setting is common in open fissures or dilatational fractures forming vein-type deposit [16].

## Methods

### Non-linear transformation

The highlight of this paper is the non-linear approach (data transformation) to handle any kinds of exploration data; mathematically expressed as the following forms [17]. The data transformation applied to all data is binary number (0, 1). However, the transformation is technically different for each data type. For instance in alteration group, value ‘1’ is given to all data ‘Smectite’ and the rest is ‘0’. The same goes with other alteration group, and so on. The threshold for this kind of data is often ‘type’, or ‘class’, or ‘classification’. Thus, the general expression of categorial data transformation is given in **Eq. 1**.

$$i_j(v_c) = \begin{cases} 1, & \text{if } v_j = v_c \\ 0, & \text{if } v_j \neq v_c \end{cases} \quad (1)$$

On the contrary, continuous data, e.g. Bi dan Mo elements in soil, will have quartiles as thresholds. For instance, on lower quartile (Q1) threshold, value ‘1’ will be given to all bismuth (Bi) and molybdenum (Mo) data above Q1, and so on. The threshold can be decile values or geochemical background value.

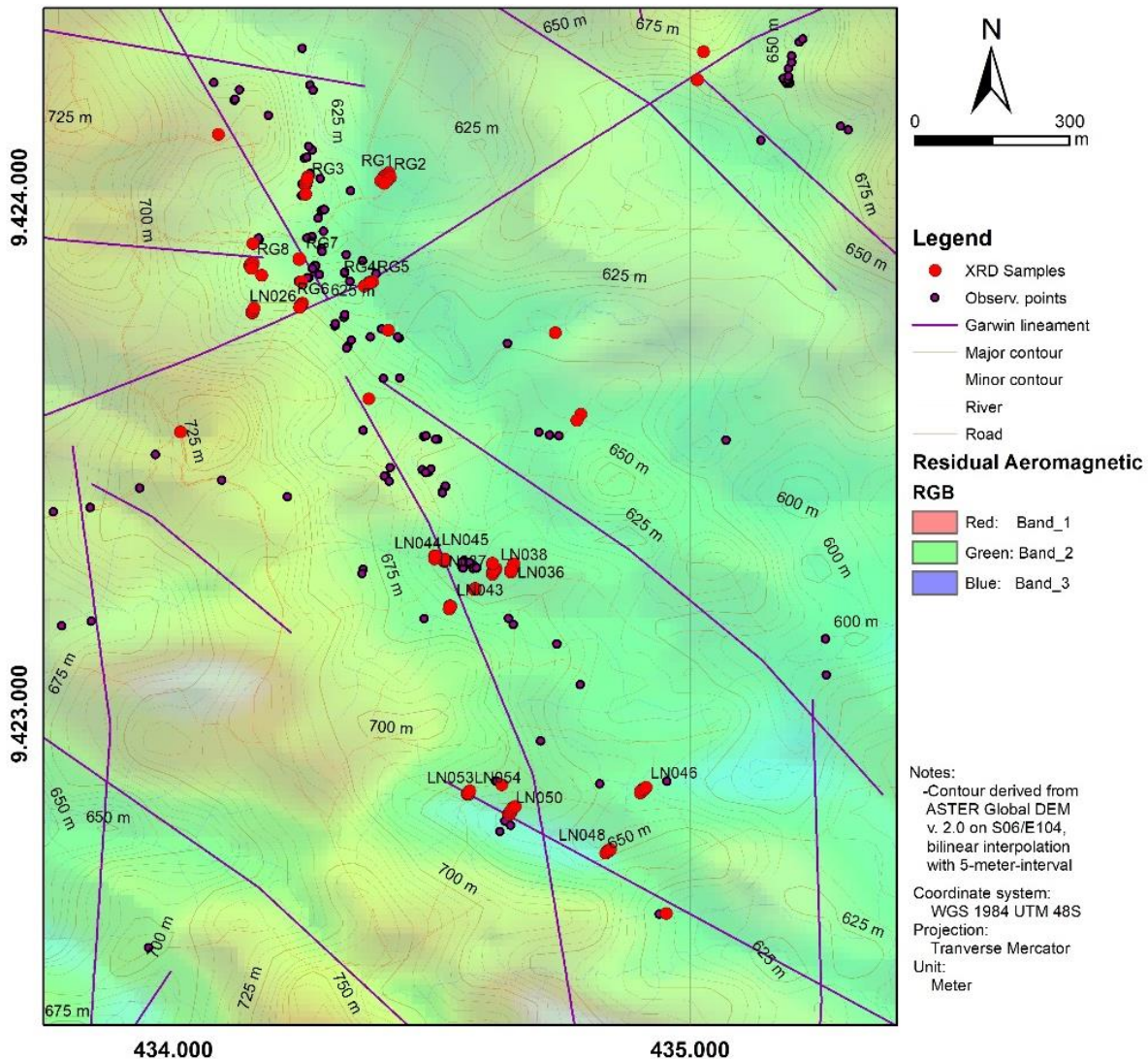


Figure 1. Observation points and XRD sampling points upon strong NW-SE lineament.

For any threshold/cut-off  $v_c$  of a set of continuous variable, datum will be transformed into indicator  $i_j(v_c)$ , using the following formula Eq. 2 [17]:

$$i_j(v_c) = \begin{cases} 1, & \text{if } v_j \geq v_c \\ 0, & \text{if } v_j < v_c \end{cases} \quad (2)$$

Therefore, using the quartile thresholds for all continuous data will be at 25%, 50%, dan 75% data, or expressed as  $i(v_{0.25})$ ,  $i(v_{0.50})$ , and  $i(v_{0.75})$ . The following table (Table 1) shows the data type as well as each thresholds the data will be assigned to.

The binary values assigned to continuous data can be treated in the opposite manner. For searching high

value/high anomaly like Bi and Mo geochemical anomaly data, the thresholds are the minimum value or cut-off grade. For treating lower value/anomaly, the thresholds are the maximum value allowed, such as ash content, sulphur content in a coal seam. The latter, value '1' will be assigned to all data below thresholds.

The alteration minerals were identified by bulk XRD, air-dried oriented XRD, and ethyleneglycol-treated oriented XRD in X-Ray Laboratory of Economic Geology, Department of Earth Resource Engineering, Kyushu University Japan. These alteration minerals were then regrouped based on typical alteration grouping for epithermal gold deposit [18], [19]; alteration mineralogy

is constrained by initially leached host-rock (by very acidic fluid, pH <2) and later neutralized by wall-rock reaction and meteoric water. Alteration minerals vary laterally and vertically. Since the study focuses on surface map, the lateral alteration mineral distribution is favored; vein-outward-wise, smectite, propylitic, and kaolinite-alunite alterations are typically found. XRD analyses out of 54 samples resulted in chlorite-smectite, propylitic, and silicification alteration – the latter is especially by the veins. Chlorite-smectite is an interlayer alteration typically transitioning smectite zone and propylitic zone in a deeper level; assemblaged from chlorite + smectite ± kaolinite ± alunite ± albite. Whereas propylitic mineral assemblage is chlorite + albite ± calcite ± smectite.

Table 1. Data transformation

Variable	Data Type	Thresholds/ cut-offs	Marginal Probability
Alteration group	Categorical	Chlorite - smectite	0.185
		Propylitic	0.504
		Silicification	0.311
Lithology	Categorical	Vein	0.512
		Andesitic tuff	0.346
		Andesitic lithic tuff	0.123
Lineament density	Categorical	Very high	0.065
		High	0.113
		Moderate	0.005
		Low	0.683
Soil elements (Bi)	Continuous	Lower quartile	0.227
		Median	0.275
		Upper quartile	0.388
		Very low	0.134
Soil elements (Mo)	Continuous	Lower quartile	1.078
		Median	1.392
		Upper quartile	2.003

A resampling was committed to lineament data at 6.6 meter interval. This was aimed to get a magnitude (length) per area of lineament, hence the lineament (length) density. The lineament density is classified into five groups - >21.58 m/m<sup>2</sup> that represents “very high length density”; 16.18-21.58 m/m<sup>2</sup> that represents “high length density”; 10.79-16.18 m/m<sup>2</sup> that represents “moderate length density”; 5.39-10.79 m/m<sup>2</sup> that represents “low length density”; and below 5.39 m/m<sup>2</sup> represents “very low length density”. These indicators or thresholds are derived based on this criterion to see how lineament will correlate to other variables.

Primary enrichments of trace elements in vein-type gold deposit include As, Ba, Bi, Mo, Pb, and Sb [20], [21]. Hence, the soil elements analysis included the mentioned elements for the clear correlation even statistically (bivariate analysis). However, Bi and Mo

have the highest correlation coefficient among others (0.701) and considered strongly correlated (positive) [22]. This Bi rise in the area reveals the positive correlation to the gold vein indicating the typical intrusion-related gold deposits [23]. To add more, both Bi and Mo are grouped into the sub-ore halo (meaning the altered rock relatively in the bottom of the deposit) as the geochemical indicators in hydrothermal gold vein deposits [24]. Different elements will be formed in every stage of orebody forming (vertically) as individual element requires a certain chemistry to stay immobile. The other elements, As, Ba, Pb, and Sb, are often featured in the near-ore halo and relatively closer to the surface (supra-ore halo) that explains why the correlations of Bi-Mo and the rest of the elements cannot come about.

**Indicator Kriging algorithm**

The non-linear Indicator Kriging general process is shown in **Figure 2**. After transforming the data, indicator variogram models are required for estimation. Indicator variogram searches for critical variance within which an area of interest or range of influence for each variables are determined. An indicator variance can guide to search the critical variance (sill). An experimental variogram has to be calculated from **Eq. 3** [25], [26] and modelled through **Eq. 4** [27], [28] based on spherical model that suits skewed data better.

$$\sum_{j=1}^{N(h)} (Y_j(x+h) - Y_j(x))^2 = 2\gamma(h) \tag{3}$$

where  $N(h)$ ,  $Y_j(x)$  and  $\gamma(h)$  are number of data pairs, data at location  $x$ , and variogram at distance  $h$  respectively. Variogram searches for variance of data pairs separated by distance  $h$ , or lag. For every indicators, variogram is calculated and hence, indicator variograms will be obtained. These experimental indicator variograms were fitted by using Matheron/spherical model in nested structure to show micro, local, and regional area of influence.

$$\gamma^{(h)}_{v_c} = \begin{cases} 0, & h = 0 \\ C_0 + C_1 \left( \frac{3|h|}{2a_1} - \frac{1}{2} \left( \frac{|h|}{a_1} \right)^3 \right) + C_2 \left( \frac{3|h|}{2a_2} - \frac{1}{2} \left( \frac{|h|}{a_2} \right)^3 \right), & 0 < |h| < a_1 \\ C_0 + C_1 + C_2 \left( \frac{3|h|}{2a_2} - \frac{1}{2} \left( \frac{|h|}{a_2} \right)^3 \right), & a_1 \leq |h| < a_2 \\ C_0 + C_1 + C_2, & |h| \geq a_2 \end{cases} \tag{4}$$

Where  $\gamma^{(h)}_{v_c}$ ,  $C_0$ ,  $C$ ,  $h$ ,  $a$ , notation 1 and 2 on **Eq. 4** stand for variogram at a threshold  $v_c$ , nugget variance, lag

distance, range, and notation representing local and regional structure, respectively.

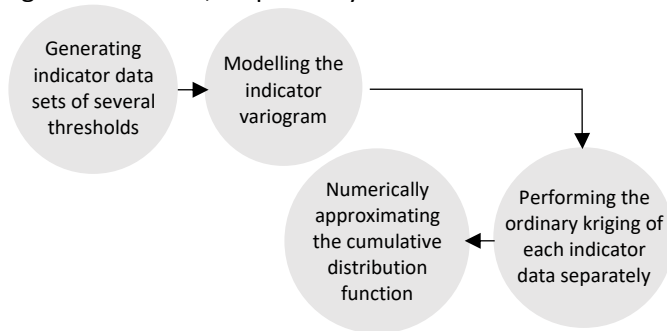


Figure 2. Non-linear Indicator Kriging algorithm.

As the thresholds are not quite the same as that of the continuous one, the term *marginal probability* will be introduced. Marginal probability works as the initial proportion of each block corresponding to each category, which is a weighed average of the sample indicators, satisfying  $\sum_{j=1}^n w_j = 1$  [29].

$$\hat{F}(v_c) = \sum_{j=1}^n w_j \cdot i_j(v_c) \quad (5)$$

Eq. 5 shows  $\hat{F}(v_c)$  and  $w_j$  stand for cumulative frequency distribution function and proportional weight at the threshold, respectively. The marginal probabilities of alteration group, lithology, lineament density, and soil element analysis are shown in Table 1. Ordinary Kriging will then be performed by the following estimator, Eq. 6,  $\hat{V}(x_0)$  at location  $x_0$  by weight  $\lambda_i$ ,

$$\hat{V}(x_0) = \sum_{i=1}^k \lambda_i V(x_i) \quad (6)$$

subject to  $\sum_{i=1}^k \lambda_i = 1$  [27]. Kriging is known as Best Linear Unbiased Estimator 'BLUE' [26]. One of the reason it is known as BLUE is due the weight  $\lambda_i$  is calculated with taking several variables into account: a) the distance between block ( $U$ )/point ( $x_0$ ) to be estimated to the sample point ( $x_i$ ); b) the distance amongst sample point ( $x_i, x_j$ ); c) and the average variance within the block to be estimated. These relationship is shown in Eq. 7 [27].

$$\sum_{i,j=1}^N \lambda_i \gamma(x_i, x_j) + \mu = \bar{\gamma}(x_j, U) \quad (7)$$

The notation  $\gamma(S_i, S_j)$ ,  $\bar{\gamma}(S_j, U)$ , and  $\mu$  refer to the value of point-to-point variogram, the average point-to-block variogram, and population mean respectively. These distances and variograms will be calculated by using the formula of fitted variogram Eq. 4 to get the  $\gamma$  values. Once weights and mean population are calculated, the estimator  $\hat{V}(x_0)$  can give the estimates in the form of **probability**. Therefore, each variable at each thresholds

will give different probability distribution or reliability map.

The last algorithm of Indicator Kriging numerically approximates the cumulative probability distribution [29]. The realization of kriging with indicator values (both continuous and categorial data) are not equiprobable because of the thresholds and marginal probabilities. In this research, realizations for categorial data will be left as probability value at a point to give easier set of values for further analyses. Whereas the realizations for continuous data will need to be estimated to give a single estimate at each point. Let  $F_x(v_j)$  be the probability at  $x$  obtained from kriging of indicator values derived from threshold  $v_j$ ,  $j = 1, 2, \dots, N$ , the conditional expectation estimator  $\hat{V}_E(x)$  that can be derived from the sets of thresholds is expressed in Eq. 8.

$$\hat{V}_E(x) \approx \sum_{j=1}^{N+1} \bar{v}_j [F_x(v_j) - F_x(v_{j-1})] \quad (8)$$

Where  $\bar{v}_j$  is the mean of the class  $(v_{j-1}, v_j)$  with  $v_0$  representing the lowest sampling value and  $v_{n+1}$  the largest.

## Results And Discussion

Geostatistics has the ability to assign confidence interval to every estimates. It does not give a single estimate but along the range or error, derived from the cumulative distribution of the random function. Once cumulative distribution is known, the confidence limit chosen to employ in this study case is a practical 'threshold probability map' showing the fluctuations in the probability that the attribute is limited to a value [29]. The limit metioned earlier is 'above', not 'below' a certain threshold because data were transformed in that manner. This threshold probability map from this point will be addressed as reliability map.

### Outstanding features of non-linear indicator variogram models for drawing surface maps

The indicator variogram models for each indicators are shown in Figure 3 and Figure 7; referring to categorial data and continuous data respectively. These indicator variogram models show the area of influence which attributes are still correlated spatially within (Table 2). An attribute comprises local area of influence (yellow shading) and regional area of influence (blue shading) indicating range of an attribute that has more similarity at a distance. For instance, propylitic alteration amongst alteration group (Figure 3a) has the most distant range;

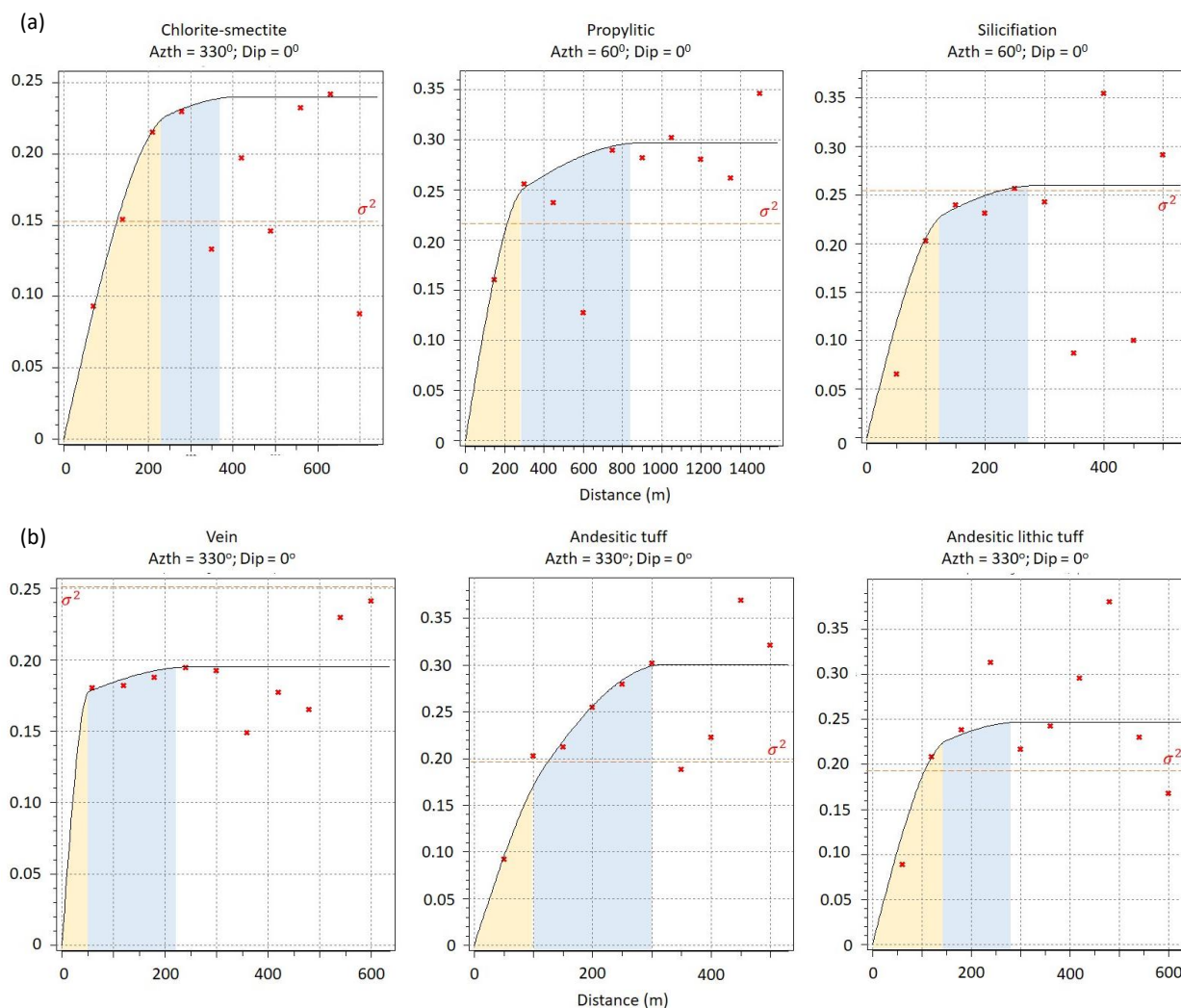


**Figure 3.** Indicator variogram models of categorical data; (a) alteration group and (b) lithology, at each thresholds.

exceeding 800m. Theoretically, this range shows that propylitic data is similar/connected upto this point. Genetically, this shows the occurrences of propylitic as the 'peripheral' alteration that surrounds other alteration halos.

**Table 2.** Variogram parameter of categorical data; local and regional range.

Variable	Thresholds/cut-offs	Local (m)	Regional (m)
Alteration group	Chlorite - smectite	245	415
	Propylitic	300	900
	Silicification	130	290
Lithology	Vein	48	250
	Andesitic tuff	120	325
	Andesitic lithic tuff	180	300

Another example from **Figure 3b**, vein has a distinct variogram model than other in terms of how erratic the

data are, shown by sudden flatness at a relatively close distance to the origin (in this case <50m). This erratic behaviour near the origin is often called nugget effect, or if very random, pure nugget. The nugget effect is so high that if the value is compiled to  $C_0$ , the estimation process will be flopped, many grids would not have been smoothed and would have been spotted. The solution is to make local range ( $a_1$ ) and local sill ( $C_1$ ) to represent the nugget effect. Resulting in no micro structure but very high variance of data at local structure. This characteristics of vein erraticness can be explained genetically; as vein occurs in an open fissure and not bulks, we will find an alternating findings of 'vein' and 'no-vein' at close distance in field.

Erratic vein data is not only in the form of the existence of vein itself, but also when Au-grade is taken account into. Au-grade is so erratic – someplaces very high and someplaces very low, or very high and low grades in the same place. This randomness also creates nugget effect – even pure nugget.

The lineament density data are so vast, regular, and small gridded that the indicator variogram will show minimum variance at every lag increase (

**Figure 4).** Because of this data nature, the lineament density will show little to no difference to the raw data distribution. An ordinary kriging or inverse distance weighing will result similarly with this kind of data, except it is categorial data. Therefore, an RGB-based lineament density is converted to somewhat representative value of very high to very low (1-5). This process is the non-linear transformation for this data

and resulted in the same reliability map, that is probability distribution map – for the purpose of finding correlation coefficient between variables easily with bivariate analysis.

The critical variance where local and regional range ends is called sills (y-axis). This variogram parameter reaches its stationarity when data is only correlated statistically. The sill should be around where the statistical variance be – that is why on the variogram model figures, dashed red line are presented showing  $\sigma^2$ . Especially for the continous data, spatial correlation can be further analysed by *multi-indicator kriging* utilizing sill values to get micro, local, and regional relationship of soil elements. This topic can be the near-future work to better understanding the methods for doing variable pairings in non-linear kriging.

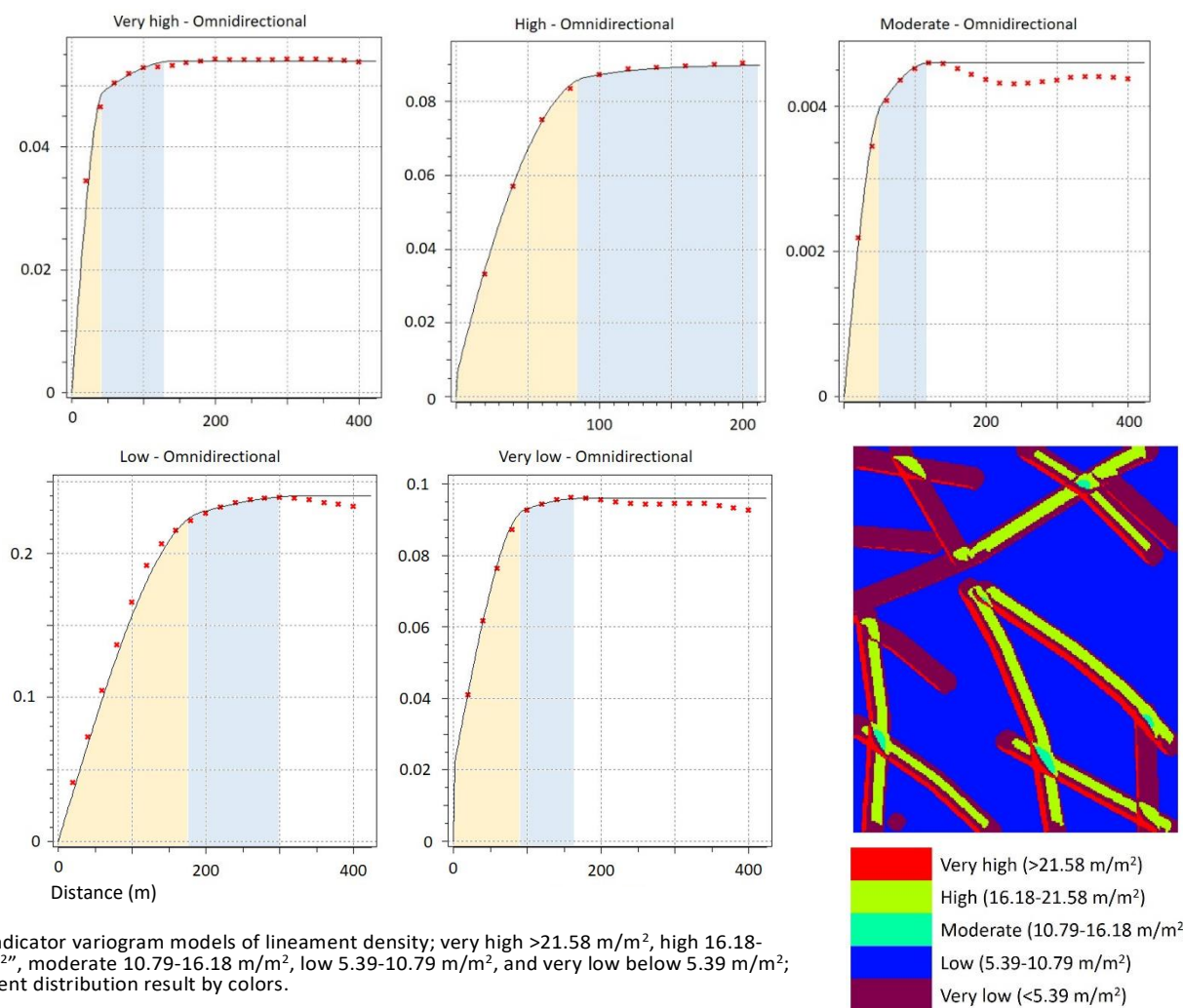


**Figure 4.** Indicator variogram models of lineament density; very high >21.58 m/m<sup>2</sup>, high 16.18-21.58 m/m<sup>2</sup>, moderate 10.79-16.18 m/m<sup>2</sup>, low 5.39-10.79 m/m<sup>2</sup>, and very low below 5.39 m/m<sup>2</sup>; the lineament distribution result by colors.

## Original Article

e-ISSN: 2581-0545 - <https://journal.itera.ac.id/index.php/jsat/>



The correlation between categorical data is further shown by the correlation coefficient at clipping values (Figure). With alteration, lithology, and lineament density, it is hard to tell the relationship aside from subjectively through genesis and occurrences of minerals. However, non-linear indicator kriging gives a range of probability value that can be easily compared one another with scatter plot. Using the marginal probability value as lower clipping value, these spatial correlation can be quantified.

### Updating local geological map

The conventional method will mostly rely on engineer's justification and experience when drawing a lithology contact when two nearest points have different lithology type. Although those justification and experience are still totally needed, now more scientifically justified data are provided to better surface map. Taking into account other attributes and how they correlate with each other. The correlation is expressed in probability values that each block has a probability for being chlorite-smectite, propylitic, or silicification (in terms of alteration group) and also a probability for being vein, andesitic tuff, or andesitic lithic tuff (in terms of lithology type).

The local geological maps derived from probability maps will consist of alteration distribution (Figure 5) and lithology maps (Figure 6), including the lineament density, sample points, and structural measurement (veins and stockworks). The alteration distribution is reflected from the probability maps a) chlorite-smectite, b) propylitic, and c) silicification alterations. All three maps are built in the same cartesian grid to easily compare the probability values between the three. An alteration of which probability is the largest will be chosen as *the identity of a grid*. Another consideration is that although a probability is the largest, if it is no larger than its marginal probability, the other probability values have to be evaluated further. This process shows that every grid has the chance to become a type of alteration by having three values of probability. This determination helps engineers to rise confidence in valuating alteration and lithology contact.

A company mined out the central and northern parts of the contract of work by 2019-2020. Being yet to be a prospect, this study area (Rawa Gabus) does not have that many detailed geological information, except for

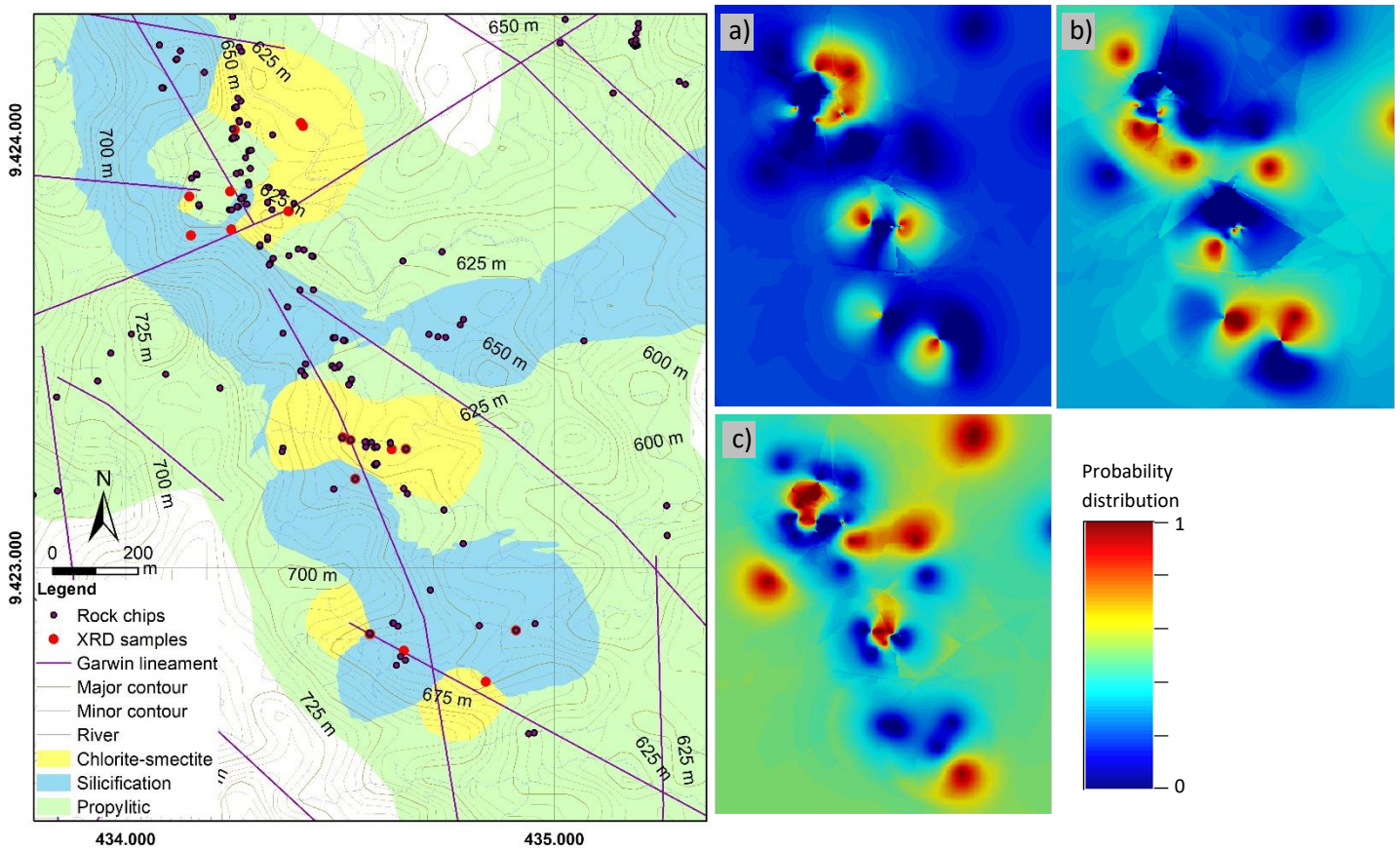
lineaments from 2012 researches. The lithology distribution is derived from probability distribution map of a) vein, b) andesitic tuff, and c) andesitic lithic tuff. All three maps are indifferent from alteration grid that each grid have more data stored. A grid in lithology type Indicator Kriging estimation will have possibilities to be either vein, andesitic tuff, or andesitic lithic tuff based on their probability values. After determining lithology grid identity, result shows the distribution as illustrated in Figure 6. Vein illustrated in the map represents the vein zones showing the surface outcrop distribution zone(s). The linkage of each zones are interpreted based on the orientation (strike/dip) plotted in the same frame. This vein zone represent neither lateral nor vertical continuation of the vein. Nevertheless, this zoning can be used to rise the confidence about vein distribution and further drilling bearing and dip decision. The former geological map created in 2018 only shows andesitic tuff throughout the frame. As the data point increased, megascopic observation set andesitic lithic tuff apart from andesitic tuff.

The significance of defining detailed lithology data to separate lithic tuff from tuff is regarding the genetic process of the volcanogenic pyroclastics. Different from the term "crystal" that is derived from porphyritic magma and from crystalline or porphyritic country rock, the term "lithic" refers to fragments or clasts derived from pre-existing rocks, including both volcanic and non-volcanic types. In general, but not invariable, lithic fragments are absent or sparse in lava flows and syn-volcanic intrusion.

The kinds of fragments in the volcanic rock as the host of the gold mineralization may imply to different contributions to vein textures, e.g. hydrothermal breccia, colloform, banded vein, etc. As the vein textures are limited to the surface outcrops, the mapping result cannot explore this matter, let alone the mineralization. Rather, the discussion can progress to whether the alteration and/or geochemical anomalies are more controlled by another factor, for instance morphology or structures. Hydrothermal alterations are various yet similar, depending on the nature and chemistry (site-specific fluid composition, fluid characteristics, and fluid concentration), temperature and pressure of the circulating fluid, as well as the permeability and initial composition of the host rocks through which the fluids circulate [30]. Thus, by updating geological map into more detailed lithology unit might help better understand the vein regimes, host rocks, and magma-fluid interaction (alteration) forming the ones we see today.



## Original Article

e-ISSN: 2581-0545 - <https://journal.itera.ac.id/index.php/jsat/>

**Figure 5.** Interpreted lateral distribution of alteration map derived from non-linear indicator kriging; resulted from analysing probability distribution map of a) chlorite-smectite, b) propylitic, and c) silicification alterations.



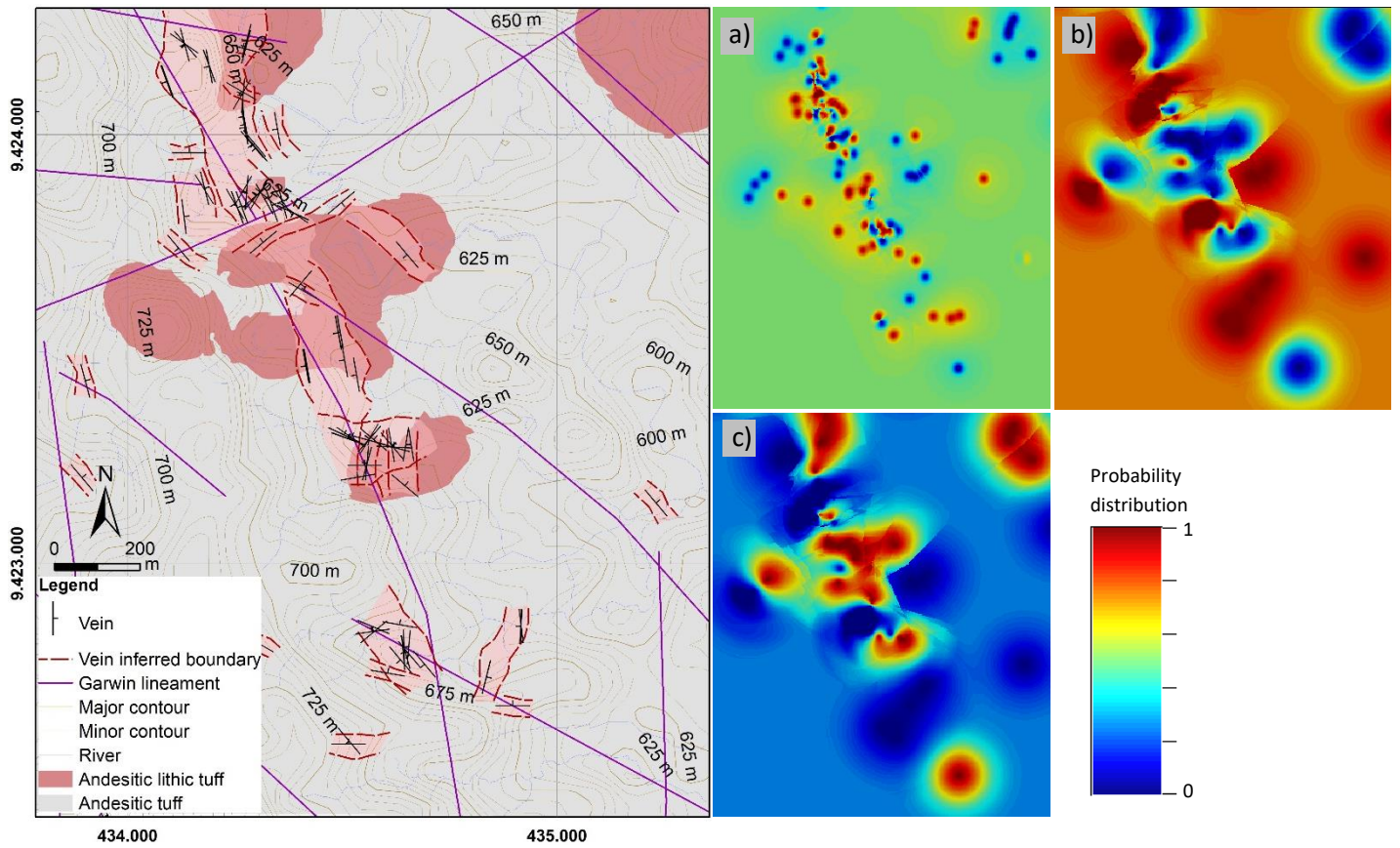


**Figure 6.** Updated geological map of research area, interpreted from non-linear indicator kriging; resulted from analysing probability distribution map of a) vein, b) andesitic tuff, and c) andesitic lithic tuff.

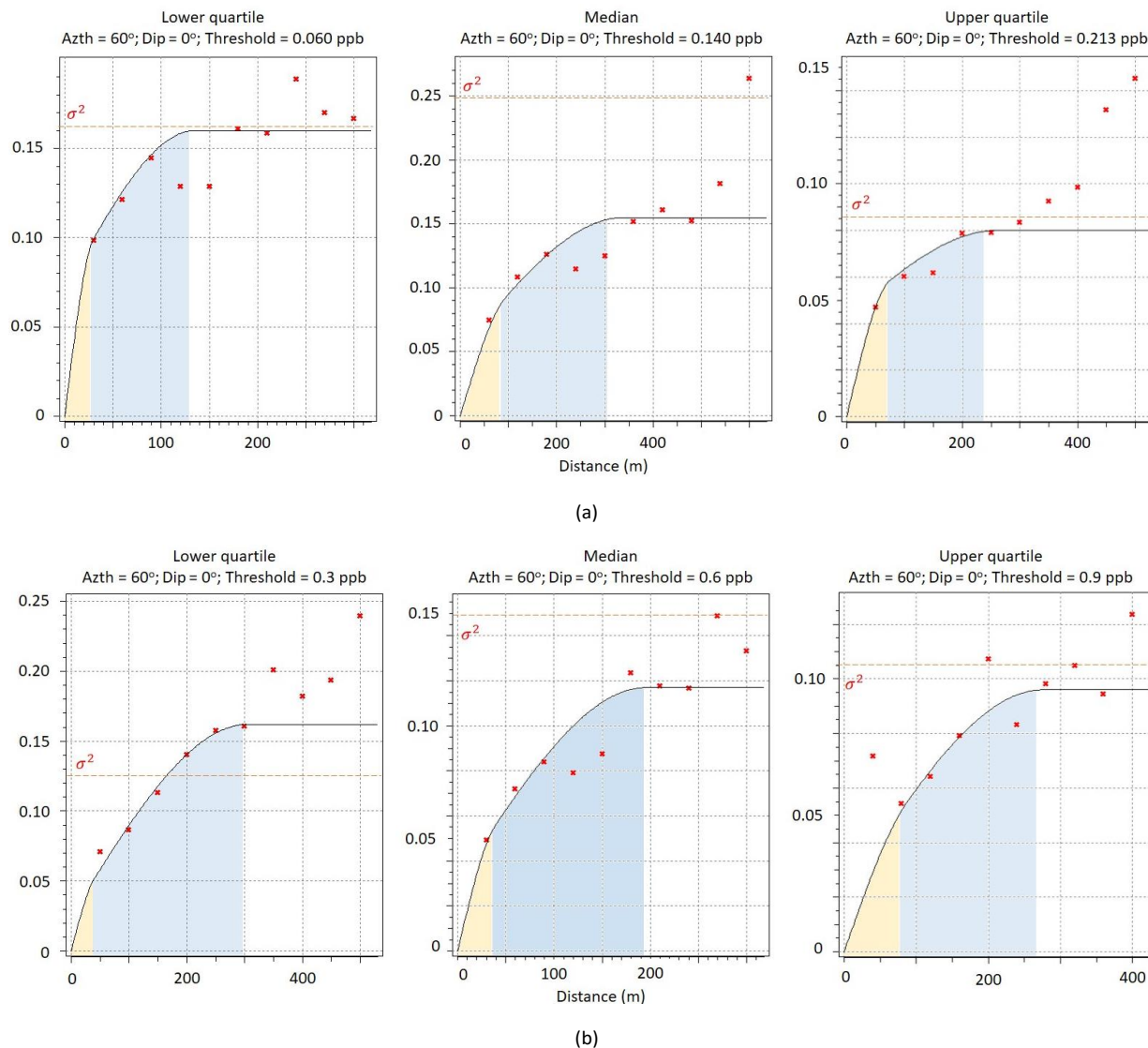


**Figure 7.** Indicator variogram models of continuous data; (a) bismuth/Bi and (b) molybdenum/Mo, at each quartile thresholds.

Magma-fluid interaction can be seen through the alteration mineral itself. An alteration mineral shows the pH range as well as temperature range which the mineral was formed in. The pH and temperature infer to the hydrothermal fluid. The alteration mineral group is matched with genetic epithermal alteration model. The wall rock alteration in epithermal system is theoretically formed as halos to vein; occurs as silicification minerals, sericite (illite) to graded peripheral smectite clays with associated pyrite and chlorite, and this alteration grades to more marginal chlorite-carbonate (propylitic) alteration. Overall distribution of alteration is along the vein zone and SE-NW lineament (visually),

especially the silicification zone. Low temperature acid water developed by the condensation of volatiles contribute towards the formation of surficial acid sulphate alteration, or known as near-surface waters, including silica (chalcedony, opal), kaolinite, and local alunite. These acid sulphate water is interpreted to collapse to deeper levels and so aid in mineral deposition. The distribution of propylitic in this study is vast, almost covers and surrounds the other alterations. Whereas the distribution of chlorite-smectite is more localised.

#### Spatial correlation

Spatial correlation amongst variable and between variables will be provided to further understand the interpreted map. Spatial correlations is only possible because indicator kriging result for any kinds of variables are their probability values, or reliability maps, which makes it easier to compare (**Table 3**). Alteration group pairs have overall negative correlation coefficients; namely propylitic and silicification, chlorite-smectite and silicification, also chlorite-smectite and propylitic have reciprocally moderate correlation (-0.62) and reciprocally strong correlation for the rest (0.71 and 0.76 at clipping values), respectively. Reciprocally correlated means alteration variables are inversely related or when one presents, the other doesn't. It is too early to conclude whether there is no replacement on the system yet. However, it is proven that the probability values representing the presence of of alteration group do not co-exist with the others.

**Table 3.** Corellation coefficients of variable pairs.

Pairs		$\rho$	Clipping values	
1	2		1	2
Chlorite-smectite	Silicification	-0.71	0.50-0.58	0.42-0.50
Chlorite-smectite	Propylitic	-0.76	0.90-0.99	0.01-0.10
Propylitic	Silicification	-0.62	-	-
Vein	Andesitic tuff	0.51	0.30-0.70	0.47-0.52
Vein	Lithic tuff	-0.12	0.30-0.47	0.48-0.58
High	Very low	0.97	0.17-0.25	0.50-0.60
High	Very low	-0.86	0.05-0.30	0.30-0.50
High	Moderate	-1.00	-	-
Low	Moderate	0.99	-	-
Low	Very high	0.85	-	-
Low	Very low	-0.76	0.01-0.25	0.25-0.50
Moderate	Very high	0.86	-	-
Moderate	Very low	-0.91	0.05-0.15	0.30-0.50
Very high	High	-0.87	0.01-0.20	0.30-0.51
Very high	High	0.90	0.25-0.42	0.50-0.60

A contrast is shown in lithology relations. There is a noticeable difference of coefficient correlation between vein and andesitic tuff and between vein and andesitic lithic tuff; the former having moderate correlation (0.51 at clipping values), the latter having little to no correlation (0.12). It is obvious that andesitic tuff has the dominance in lithology distribution that such value is reasonable. Various coefficient correlations are potrayed amongst lineament density pairs; *strong reciprocal relationship* between very high – high (-0.87), moderate – very low (-0.91), low – very low (-0.76), high – moderate (-1.0), and high – very low (-0.86) lineament density at clipping values. Lineament densities were classified base on its RGB values with no overlaps in the first place that this reciprocal relation is expected.

Elseways, some lineament density pairs have *strong positive correlation*, namely high – very low (0.97), low – moderate (0.99), low – very high (0.85), moderate – very high (0.86), and high – very high (0.90) at clipping values. In this case, positive relation was required because the increasing or decreasing probability value at the same grid is mutual.

### Soil elements geochemical anomaly and background

The transformed value of soil element is treated in 'minimum' manner – meaning data above threshold are converted into 1, as the rest is 0. For this research, continous data thresholds are the quartile values. The results will be compared to linear geostatistics as Ordinary Kriging and conventional method inverse distance weighing.

After variogram models for each quartile have been obtained (**Figure 7**), the estimation algorithm will calculate as three separate parts; namely *probability distribution of a soil element having higher value than threshold lower quartile, median, and upper quartile*. All these values are still like puzzle pieces with no real value (in ppb) of the soil element concentration. Converting a probability value from a cell in a certain threshold has to be weighed with the sample means at each thresholds; the mean of upper 75% raw data for lower quartile, the mean of upper 50% raw data for median, the mean of upper 25% raw data for upper quartile, with data sorting. The sample means of bismuth (Bi) used at lower, median, upper quartile weighs are 0.277, 0.275, and 0.388 respectively. Whereas the sample means of molybdenum (Mo) used at lower, median, upper quartile weighs are 1.078, 1.392, and 2.003 respectively.

The continous data treated with Indicator Kriging will show several results that can be easily distinguished statistically. The histograms on **Figure 8** shows the change from original data to the estimated value. Typically, Ordinary Kriging (OK) will make the lower values higher and the higher values lower to create 'smoothing effect' or to create lower variance, living up to its name 'BLUE'. This phenomenon is shown in Mo results. Meanwhile, the smoothing does give a rise on mean value, as Bi mean value rise from 0.189 to 0.221 ppb; and Mo mean value rise from 0.942 to 1.595 ppb (

**Table 4**). The Ordinary Kriging was done in the similar direction with Indicator Kriging (azimuth N 60° E) and similar angle of tolerance (45°). This shows more advantage of Kriging method to justify estimation result not only statistically, but also the spatial data distribution.

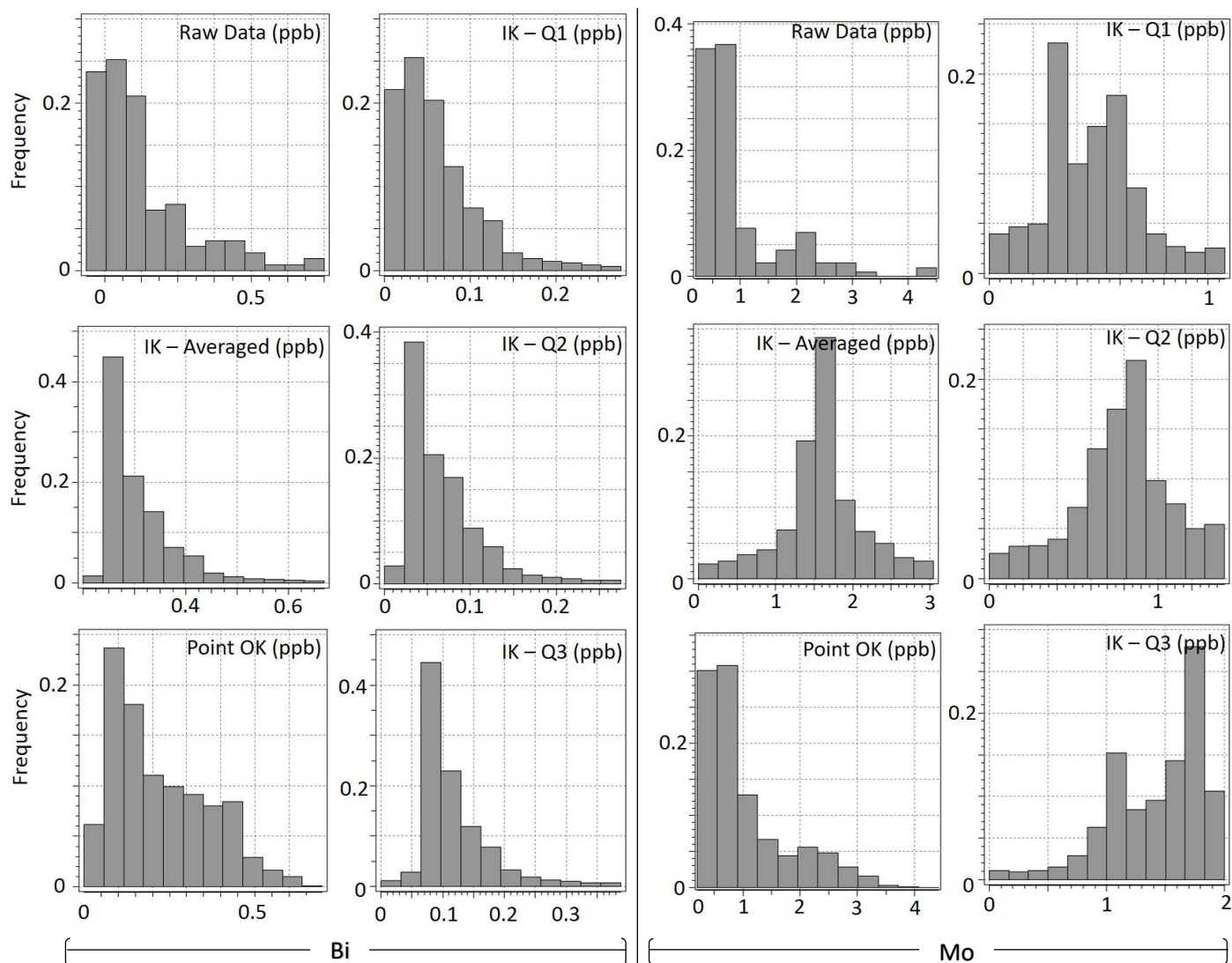


**Figure 8.** Histograms of raw data, indicator kriging and ordinary kriging results; left – bismuth (Bi), right – molybdenum (Mo).

**Table 4.** Comparisons of geostatistic methods on continuous data.

Statistical summary	Bi		Mo	
	Mean	Variance ( $10^{-2}$ )	Mean	Variance
Raw data	0.189	1.988	0.942	0.658
IK – Threshold Q1	0.061	0.228	0.469	0.046
IK – Threshold Q2	0.068	0.181	0.782	0.086
IK – Threshold Q3	0.117	0.331	1.425	0.169
IK - Averaged	0.226	1.898	1.595	0.294
Ordinary Kriging (OK)	0.221	2.013	1.044	0.537

Abbrev. : IK – Indicator Kriging, OK – Ordinary (point) Kriging, Q1 to Q3 – lower, middle, and upper quartile respectively.

Averaged Indicator Kriging means the value weighed from its probability values in each quartiles. Multiplying the probability value at each grids with the mean quartile, gives the sense of which quartile the data is more normally distributed and/or similar to its raw data characteristics (**Figure 8**). The first columns of both elements show the tiny data shift to the right (less skewed to the right). Especially the averaged indicator kriging of Mo resulted in very much normal distribution. However, the ordinary kriging for the same Mo data does not result similar data distribution. This phenomenon is supported by the variance drop of Mo estimated with averaged indicator kriging ( $0.294 \text{ ppb}^2$ )

than that of raw data (0.658) and ordinary kriging (0.537 ppb<sup>2</sup>). The result for Bi does not show the contrast variance drop, the cause is *inferred* to the data nature of Bi that is very skewed to the right (positive skewness or few data with much higher values). The second column of each elements shows the shift of indicator kriging results of lower, middle, and upper quartiles. The Bi shifts are not as progressive as Mo shifts; proving that the Bi data is much more skewed than Mo data.

Geochemical anomaly is calculated analytically by mean and standard deviation values. What separates background and anomaly now is the confidence level for each data; the greater the confidence level is, the certainty to call some values anomalies is higher. Otherwise, the lower the confidence level is, the anomaly range should be widened to accommodate the uncertainty. In this case study, anomaly values for raw data, averaged indicator kriging, and ordinary kriging of Bi are similar; a) from 0.330 ppb, 0.364 ppb, and 0.363 ppb up respectively, at 95% confidence level; b) from 0.388 ppb, 0.421 ppb, and 0.422 ppb up respectively, at 90% confidence level. Meanwhile, The Mo anomaly values are lower when estimated with ordinary kriging; affected by the effective smoothing from the method.

## Conclusions

Non-linear indicator kriging provides 'threshold probability maps' that not only covers continuous data but also categorical data. The categorical data can be transformed into geological features; lineament density, lithology, alteration to update the previous maps in spatially analysed manner. Spatial correlation can be obtained only because both categorical data and continuous data are presented by their probability values. Now the correlation between variables can be quantified, and not subjectively by engineer's justification although this correlation must be proven further in the field. Analysing data in the same grid will have many advantages in terms of data management; all data in an exact-same-size-box. Indicator kriging for continuous data shows its flexibility to be treated in the 'minimum' or 'maximum' manner. Beside, the flexibility of which data percentages the engineer will use can be adjusted – not only by its quartile values, but also deciles, and many more. Indicator kriging for continuous data will not only show this flexibility, but also lower the estimation variance like ordinary kriging does.

## Acknowledgements

All laboratory analysis were provided and funded by JASSO Scholarship in Kyushu University Laboratorium of Economic Geology. The field data acquisition was not impossible because of PT Natarang Mining's will to provide enormously.

## Conflict of Interest

There are no conflicts to declare.

## References

- [1] S. K. Haldar, "Photogeology, Remote Sensing and Geographic Information System in Mineral Exploration," in *Mineral Exploration*, Elsevier, Inc., 2013, pp. 95–115.
- [2] R. J. Durrheim, M. S. D. Manzi, and S. J. Webb, "Exploration Geophysics," in *Encyclopedia of Geology*, 2nd ed., D. Alderton and S. A. B. T.-E. of G. (Second E. Elias, Eds. Oxford: Academic Press, 2021, pp. 219–234.
- [3] D. Müller, K. Kwan, and D. I. Groves, "Geophysical implications for the exploration of concealed orogenic gold deposits: A case study in the Sandy Lake and Favourable Lake Archean greenstone belts, Superior Province, Ontario, Canada," *Ore Geol. Rev.*, vol. 128, p. 103892, 2021.
- [4] A. S. Macheyeke, X. Li, D. P. Kafumu, and F. Yuan, "Elements of exploration geochemistry," in *Applied Geochemistry: Advances in Mineral Exploration Techniques*, Elsevier, Inc., 2020, pp. 1–43.
- [5] A. M. Evans, *Introduction to mineral exploration*, 2nd ed. Oxford, UK: Blackwell Publishing, 2006.
- [6] S. M. Gandhi and B. C. Sarkar, "Chapter 7 - Geological Exploration," in *Essentials of Mineral Exploration and Evaluation*, S. M. Gandhi and B. C. B. T.-E. of M. E. and E. Sarkar, Eds. Elsevier, 2016, pp. 159–198.
- [7] A. J. Sinclair and G. H. Blackwell, *Applied Mineral Inventory Estimation*. Cambridge: Cambridge University Press, 2004.
- [8] S. K. Haldar, "Mineral Resource and Ore Reserve Estimation," in *Mineral Exploration: Principles and Application*, 2nd ed., Elsevier, Inc., 2018, pp. 145–165.
- [9] d. g Krige, *Statistical applications in mine valuation*. 1962.
- [10] S. K. Haldar, "Chapter 9 - Statistical and

- Geostatistical Applications in Geology,” in *Mineral Exploration*, S. K. B. T.-M. E. (Second E. Haldar, Ed. Elsevier, 2018, pp. 167–194.
- [11] S. KASMAEE, J. GHOLAMNEJAD, A. YARAHMADI, and H. MOJTAHEDZADEH, “Reserve estimation of the high phosphorous stockpile at the Choghart iron mine of Iran using geostatistical modeling,” *Min. Sci. Technol.*, vol. 20, no. 6, pp. 855–860, 2010.
- [12] K. Saikia and B. C. Sarkar, “International Journal of Coal Geology Coal exploration modelling using geostatistics in Jharia coal field, India TO GO RAILWAY STATION,” *Int. J. Coal Geol.*, vol. 112, pp. 36–52, 2013.
- [13] E. Pardo-igúzquiza, P. A. Dowd, J. M. Baltuille, and M. Chica-olmo, “International Journal of Coal Geology Geostatistical modelling of a coal seam for resource risk assessment,” *Int. J. Coal Geol.*, vol. 112, pp. 134–140, 2013.
- [14] S. M. Gandhi and B. C. Sarkar, “Geostatistical Resource/Reserve Estimation,” in *Essentials of Mineral Exploration and Evaluation*, Elsevier, Inc., 2016, pp. 289–308.
- [15] M. Z. Abzalov and M. Humphreys, “Resource Estimation of Structurally Complex and Discontinuous Mineralization Using Non-linear Geostatistics : Case Study of a Mesothermal Gold Deposit in Northern Canada,” *Explor. Min. Geol.*, vol. 11, no. 1–4, pp. 19–29, 2002.
- [16] G. D. Faye, A. Yamaji, K. Yonezu, T. Tindell, and K. Watanabe, “Paleostress and fluid-pressure regimes inferred from the orientations of Hishikari low sulfidation epithermal gold veins in southern Japan,” *J. Struct. Geol.*, vol. 110, no. October 2017, pp. 131–141, 2018.
- [17] E. H. Isaaks and R. M. Srivasta, *An Introduction to Applied Geostatistics*. New York: Oxford University Press, 1989.
- [18] J. W. Hedenquist, Y. Matsuhisa, E. Izawa, N. C. White, W. F. Giggenbach, and M. Aoki, “Geology, geochemistry, and origin of high sulfidation Cu-Au mineralization in the Nansatsu district, Japan,” *Econ. Geol.*, vol. 89, no. 1, pp. 1–30, 1994.
- [19] N. C. White and J. W. Hedenquist, “Epithermal Gold Deposits: Style, characteristics, and exploration,” *Society of Economic Geologists Newsletter*, pp. 9–13, Oct-1995.
- [20] D. P. Cox and W. C. Bagby, “Descriptive model of Au-Ag-Te veins,” *Mineral Deposit Models, US Geol. Surv. Bull.*, vol. 1693, p. 124p, 1986.
- [21] W. Khant, I. W. Warmada, A. Idrus, L. D. Setijadji, and K. Watanabe, “Geochemical Characteristics of Host Rocks of Polymetallic Epithermal Quartz Veins at Soripesa Prospect Area, Sumbawa Island, Indonesia,” *Procedia Earth Planet. Sci.*, vol. 6, pp. 30–37, 2013.
- [22] D. J. Rumsey, *Statistics for Dummies*, 2nd ed. Canada: Wiley Publishing, Inc., 2011.
- [23] R. R. Rowe and X. Zhou, “Models and exploration methods for major gold deposit types,” in *Proceedings of exploration*, 2007, vol. 7, pp. 691–711.
- [24] C. Wang *et al.*, “Characterization of primary geochemical haloes for gold exploration at the Huanxiangwa gold deposit, China,” *J. Geochemical Explor.*, vol. 124, pp. 40–58, 2013.
- [25] M. P. Barnes, *Computer-assisted mineral appraisal and feasibility*. Society for Mining Metallurgy, 1980.
- [26] M. Armstrong, *Basic Linear Geostatistics*. New York: Springer-Verlag Berlin Heidelberg, 1998.
- [27] G. Matheron, “Theory of regionalized variables and its applications,” *Cah. Cent. Morphol. Math.*, vol. 5, p. 211, 1971.
- [28] G. Matheron and C. D. M. Mathematique, “The intrinsic random functions and their applications,” vol. 5, no. March 1973, pp. 439–468, 1973.
- [29] R. A. Olea, *Geostatistics for engineers and earth scientists*, 3rd ed. New York: Springer Science & Business Media, 2012.
- [30] F. Pirajno, *Hydrothermal processes and mineral systems*. Springer Science & Business Media, 2008.